Remote Sensing of Environment 158 (2015) 15–27

Contents lists available at ScienceDirect

Remote Sensing of Environment

journal homepage: www.elsevier.com/locate/rse

Quantifying forest canopy traits: Imaging spectroscopy versus field survey

Gregory P. Asner *, Roberta E. Martin, Christopher B. Anderson, David E. Knapp

Department of Global Ecology, Carnegie Institution for Science, 260 Panama Street, Stanford, CA 94305, USA

ARTICLE INFO

Article history:
Received 16 June 2014
Received in revised form 13 November 2014
Accepted 14 November 2014
Available online 5 December 2014

Keywords:
Amazon basin
Canopy chemistry
Carnegie Airborne Observatory
Chemometrics
Data fusion
Hyperspectral
LiDAR
Tropical forest

ABSTRACT

Spatial and temporal information on plant functional traits are lacking in ecology, which limits our understanding of how plant communities and ecosystems are changing. This problem is acute in remote tropical regions, where information on plant functional traits is difficult to ascertain. We used Carnegie Airborne Observatory visible-to-shortwave infrared (VSWIR) imaging spectroscopy with light detection and ranging (LiDAR) to assess the foliar traits of Amazonian and Andean tropical forest canopies. We calibrated and validated the retrieval of 15 canopy foliar chemicals and leaf mass per area (LMA) across a network of 79 1-hectare field plots using a new VSWIR-LiDAR fusion approach designed to accommodate the enormous scale mismatch between field and remote sensing studies. The results indicate that sparse and highly variable field sampling can be integrated with VSWIR-LiDAR data to yield demonstrably accurate estimates of canopy foliar chemical traits. This new airborne approach addresses the inherent limitations and sampling biases associated with field-based studies of forest functional traits, particularly in structurally and floristically complex tropical canopies.

1. Introduction

Plant functional diversity expresses many ecological processes ranging from natural selection to CO_2 exchange between the biosphere and atmosphere. Despite its central importance to evolutionary and ecological research, our knowledge of plant functional diversity remains very limited in space and time. Specifically, a major knowledge gap has developed between small-scale field studies (≤1 ha) of plant functional traits and broad-scale, remotely sensed estimates of vegetation properties. On the one hand, field studies provide an understanding of the inter-relationships between functional traits, and the ways that plants express those traits. In contrast, remotely sensed data from satellites have proven reliable for estimating changes in vegetation cover and structure, with far less success in measurements of functional diversity.

This scale-gap in functional ecology is exemplified in Amazonian forests. For example, an array of tree- and plot-scale studies have been undertaken to assess an important aspect of plant functional diversity — canopy chemistry (e.g., Cuevas & Medina, 1988; Fyllas et al., 2009; Reich, Ellsworth, & Uhl, 1995), yet collectively the literature has provided little spatial information on the chemical diversity of Amazon forest communities. Moreover, field-based foliar trait studies are highly susceptible to the contributions of mostly unknown, spatially-explicit environmental filters like the underlying geology and soils, and variable biological and structural diversity within and across communities, which when combined, may limit our understanding of plant functional diversity and assembly. Only one study has sampled the many thousands of Amazonian tree species required to resolve an assembly pattern of canopy chemical traits (Asner, Martin, et al., 2014), but like all other field studies, it could not provide spatially detailed information. As a result, potential changes in tropical forest functional patterns continue to go unobserved, with cascading limitations on our ability to model future changes in forest composition and functional processes (Simonson, Coomes, & Burslem, 2014).

In contrast to the limitations of field studies, remote sensing of Amazonian forests has provided spatially contiguous information over time, but the information has mostly been limited to forest cover, deforestation and disturbance (e.g., Achard et al., 2014; Souza, Roberts, & Cochrane, 2005). Far fewer studies have considered forest biomass and phenology (e.g., Baccini et al., 2012; Samanta et al., 2010), or plant community composition (Chambers et al., 2007; Tuomisto et al., 2003). None have quantitatively mapped forest canopy chemistry, leaving us with no direct way of linking leaf studies to large-scale processes or environmental gradients throughout the region.

Quantification of canopy chemical patterns in Amazonian ecosystems is needed to advance our understanding of functional biogeography, and to observe functional change over time. Given the enormous geographic extent of the Amazon region, remote sensing will be the only way to develop an understanding of changing functional diversity. However, remote sensing ultimately requires a connection to field

* Corresponding author. Tel.: +1 650 325 1521.
E-mail address: gpa@carnegiescience.edu (G.P. Asner).

http://dx.doi.org/10.1016/j.rse.2014.11.011
0034-4257/

measurements for purposes of calibration, validation and interpretation. Like most tropical forest regions, Amazonia presents a great challenge to pair field measurements with remotely sensed data (Fig. 1). Bear in mind that these forest canopies reach 40 or more meters in height on variable terrain, and are found in structurally complex assemblages comprised of thousands of species, often with no two locally neighboring trees of the same species. It is simply infeasible to sample enough of the canopy — whatever the trait of interest — in a way that directly links field and remotely sense data at a scale commensurate to large-area mapping applications. We need new remote sensing techniques that are compatible with the relatively sparse way that forests are sampled in the field.

Here we focused our functional trait work on a wide variety of forest canopy chemical compounds synthesized in leaves to support multiple, interdependent functional processes. Chlorophylls and carotenoids facilitate light capture and photo-protection. Nitrogen (N) and phosphorus (P) are required for carbon fixation, growth metabolism and nucleic acids. Metabolic elements like rock-derived macronutrients (e.g., Ca, K, Mg) and micronutrients (e.g., B, Fe) support multiple leaf functions such as carbon allocation (Demarty, Morvan, & Thellier, 1984). Soluble carbon (C) — comprised of sugars, starch and pectin — is synthesized as the initial energy store for the plant (Chapin, 1991; Evans, 1989). Leaf structural compounds including lignin and cellulose are generated to support strength and longevity, and to decrease palatability to herbivores (Melillo, Aber, & Muratore, 1982). In tropical canopies, phenolic compounds are synthesized primarily for chemical defense of leaves (Coley, Kursar, & Machado, 1993). Light capture and growth chemicals are also coordinated with variation in leaf mass per

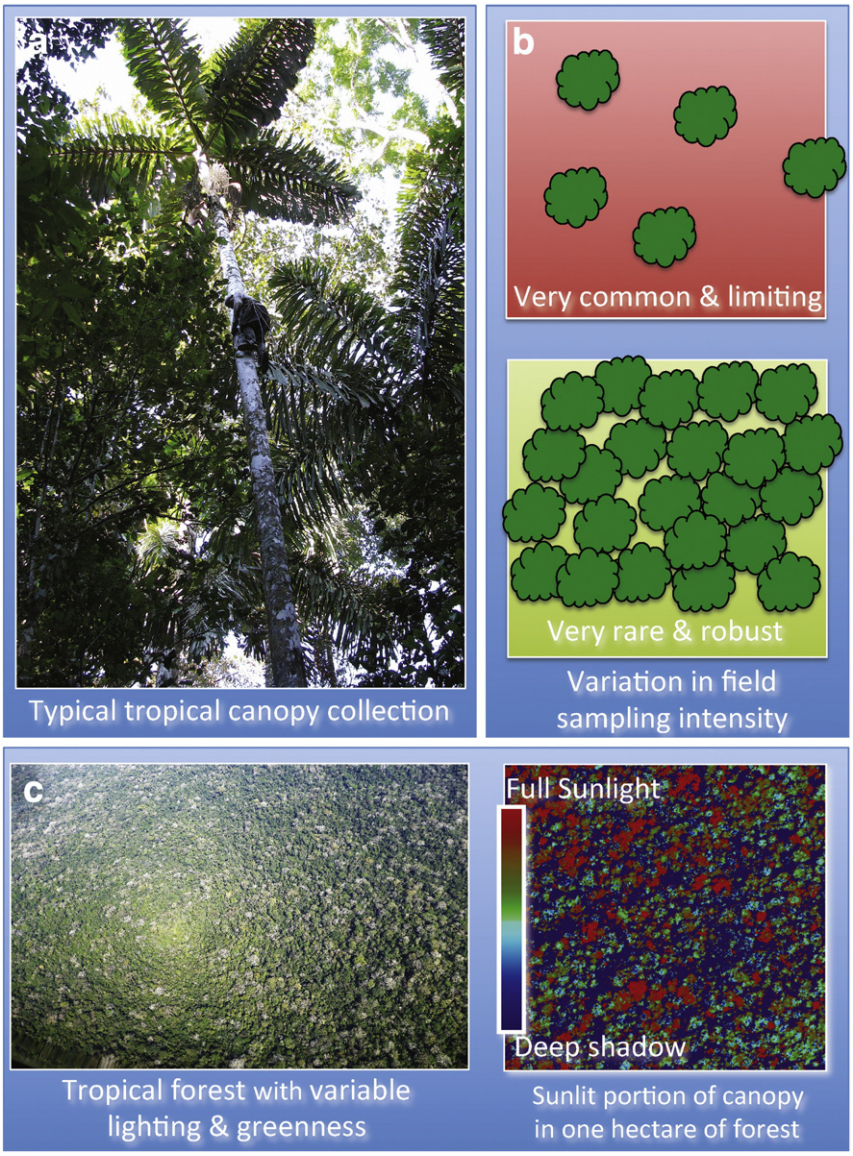

Fig. 1. There exists a fundamental mismatch between field and remote sensing studies of forest canopy traits. In tropical forests, which contain thousands of species coexisting as very tall canopies, and often in complex terrain and remote regions, fieldwork must necessarily be carried out in a tactical or selective fashion. Major sampling trade-offs exist at regional, landscape, plot, tree, branch and leaf levels. (a) In the case of canopy chemistry, individual trees such as this palm are climbed, and foliage from one or more branches is laboriously collected for transport and analysis in laboratories. (b) Field plots are sampled, often sparsely, due to issues of limited canopy access, as well as to control for vertical light gradients in the canopy that add uncertainty to canopy trait studies. Field sampling intensity, as shown here, may vary widely from plot to plot, from commonly sparse to rarely complete inventory. (c) From above, aircraft and satellite remote sensing instruments are also challenged by highly variable illumination conditions that are convolved to variable canopy structure. Additionally, some portions of most forest canopies are leafless at the time of observation, as shown in gray crowns in the aerial photography. Methods are needed to bridge the huge gap between the realities of field collection and those of remote sensing observations.

area (LMA) and water content (Wright et al., 2004). This chemical portfolio expresses multiple strategies undertaken by plants to maximize fitness over the lifetime of the individual or species.

Remote sensing of canopy chemistry has primarily been attempted with imaging spectroscopy, also known as hyperspectral imaging (Curran, 1989; Ustin, Roberts, Gamon, Asner, & Green, 2004; Wessman, Aber, Peterson, & Melillo, 1988b). Imaging spectrometers measure the solar radiation reflected from a surface in narrow, contiguous spectral channels covering a broad wavelength region (Goetz, Vane, Solomon, & Rock, 1985). Recently two contrasting viewpoints have emerged in the effort to estimate canopy chemical properties from imaging spectroscopy. On the one hand, applied studies indicate that foliar chemical traits can be estimated from spectral reflectance and absorptance features (Kokaly, Asner, Ollinger, Martin, & Wessman, 2009; Townsend, Foster, Chastain, & Currie, 2003; Ustin et al., 2009). On the other hand, modeling work suggests that the spectral signatures of plant canopies are sometimes dominated by structural variation (Knyazikhin et al., 2013), leaving it unclear as to whether canopy chemistry can be retrieved from imaging spectroscopy in the presence of these confounding effects.

In the case of forests, theory and models suggest that canopy chemistry can be estimated with imaging spectroscopy under specific measurement conditions. First, the spectrometer must be capable of acquiring high-fidelity measurements, defined by very high signal-to-noise, detector uniformity and instrument stability, to record minute variations in the spectral radiance features of vegetation (Asner & Green, 2001; Green et al., 1998). Second, there must be sufficient plant material cross-section and optical depth presented to the imaging sensor for the foliar chemical traits to be most fully expressed in the measured spectra. When canopies are optically thin, or with low leaf area index (LAI), as can be the case in water-limited environments, vegetation structure may be a more prominent contributor to reflectance than foliar chemistry (Jacquemoud et al., 2009). In contrast, LAI and canopy cover are often high in tropical forests, and optically thick canopies afford the best observing conditions for developing canopy chemical estimates from imaging spectroscopy (Asner, 2008; Atkinson, Foody, Curran, & Boyd, 2000). Nonetheless, variation in LAI has more of an effect on reflectance in the near-infrared (e.g. 800–1200 nm) than it does in the visible (400–700 nm) or shortwave-infrared (>1300 nm)

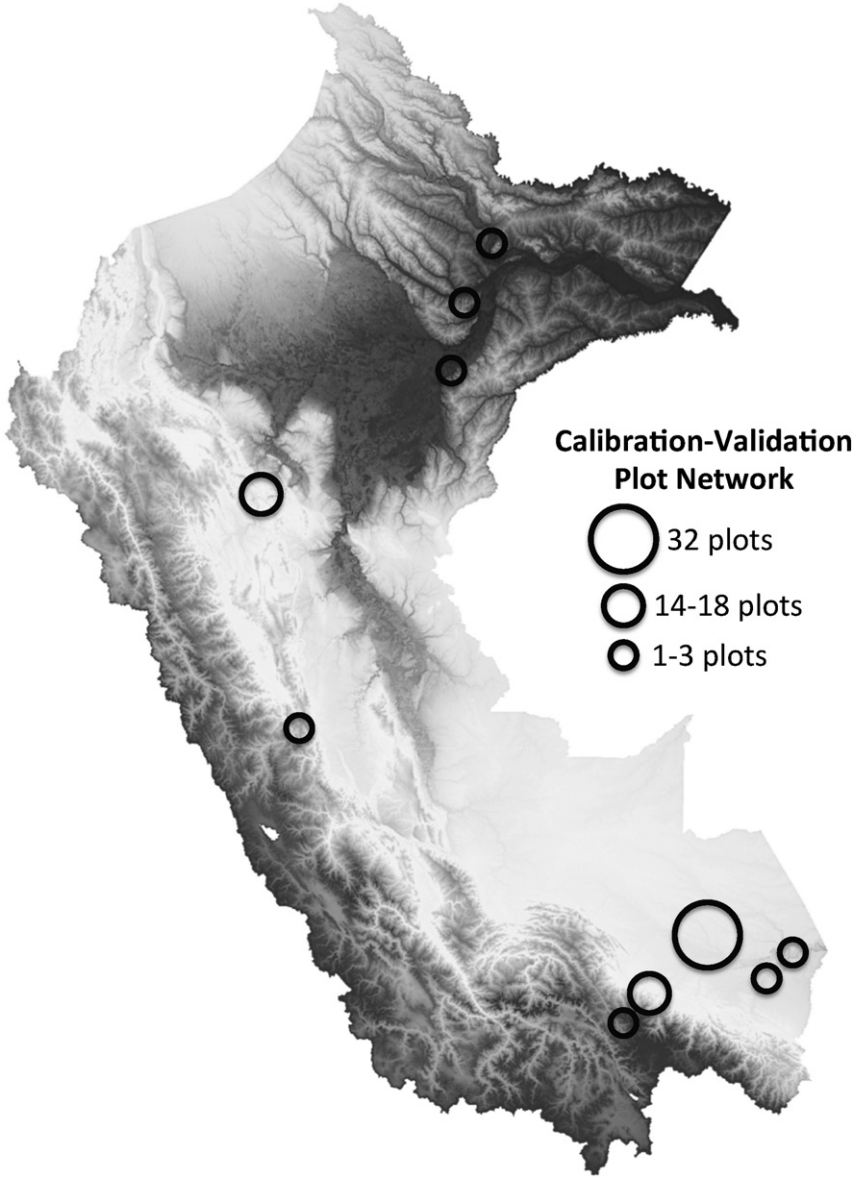

Fig. 2. Topographic map of Peru with general location (circles) of 79 1-hectare Carnegie Spectranomics Project (CSP) field plots used for calibration and validation of canopy functional traits in the Andes to Amazon region.

wavelength ranges (Myneni & Asrar, 1993), and this needs to be considered when selecting instrumentation and methods of spectral analysis. Third, the relative importance of foliar chemistry and canopy structure on the spectral reflectance signatures of canopies is spatially dependent; Intra- and inter-canopy gaps diminish the contribution of foliar chemical variation on remotely sensed reflectance (Gerard & North, 1997). Finally, the sun-to-canopy illumination and viewing conditions must be controlled for in order to extract comparable spectral signatures across images, landscapes and over time.

To address the many factors that make remote sensing of canopy chemistry difficult with imaging spectroscopy, we developed a method that links the often-sparse, field-based sampling of forest canopies with a new method for sampling the spectral properties of the canopies. We tested the method using airborne high-fidelity imaging spectroscopy along a 3000 m elevation gradient stretching from lowland Amazonia to treeline in the Peruvian Andes. With new measurements from the Carnegie Airborne Observatory — Airborne Taxonomic Mapping System, or CAO-AToMS (Asner et al., 2012), we attempted to remotely quantify 15 foliar chemicals and LMA. In doing so, we evaluated the precision and accuracy of remotely sensed foliar traits compared to those derived from field and laboratory techniques.

2. Methods

2.1. Study region

Our study incorporated field and airborne measurements from forested landscapes stretching from the western Amazonian lowlands to submontane and montane forests of the Peruvian Andes (Fig. 2). Across these landscapes, elevation increases from about 100 m to more than 3000 m above sea level. Mean annual precipitation varies <1100 to >5000 mm yr^{-1}, and mean annual temperature ranges from 13 °C to 26 °C (Table 1). Soils in the lowland landscapes range from Ultisols on clay *terra firme* (terrace) substrates to Inceptisols on alluvial floodplains, and to white sandy Entisols. In the Andean landscapes, soils are mostly classified as Inceptisols and Entisols. Vegetation at all sites is humid, broadleaf tropical forest. Canopies are densely foliated, with LAI ranging from about 3–8 (Girardin et al., 2010). Fractional intercepted photosynthetically active radiation (fIPAR) often exceeds 98% (Asner, Anderson, et al., 2014).

2.2. Field plots

Throughout the Andes-to-Amazon study region, we established 79 1-hectare field plots for use in calibration and validation of our remote sensing method (Fig. 2, Table S1). Like in most tropical forests, exceptional taxonomic and structural diversity, and canopy inaccessibility, made it infeasible to sample all tree species in our field plots. In each plot, a range of sampling intensities, from 3 to 38 trees with full sunlight canopies (Tables S2–S4), was selected for collection (Fig. 1). These plots are part of the Carnegie Spectranomics Project (CSP) network, and have been described in detail by Asner, Martin, et al. (2014). Highly variable numbers of tree collections reflect the reality of canopy access, both in terms of terrain and tree climbing.

Leaf collections were conducted using tree-climbing techniques. For each tree, two fully sunlit branches at the top of the canopy were selected and cut, sealed in large polyethylene bags to maintain moisture, stored on ice in coolers, and transported to a local site for processing within 3 h, and usually less than 30 min. A subset of fully expanded leaves was randomly selected from the branches for scanning to determine fresh leaf area, and weighing to record fresh and dry weights as well as leaf water concentration. Additional leaves were selected for oven drying at 70 °C and another for acquisition of fresh leaf disks to be immediately frozen to -80 °C in liquid N. Both subsets were maintained in their stabilized state for subsequent chemical analyses in the Carnegie Spectranomics Library, Stanford, CA, USA. Values of fresh leaf area were divided by dry weight to determine LMA. The protocol for scanning, water, and LMA determination is provided on the CSP website (http://spectranomics.ciw.edu).

Laboratory protocols for all chemical assays were given by Asner and Martin (2011) and Asner, Martin, et al. (2014), and see http://spectranomics.ciw.edu. A brief overview is provided here. Dried leaves were ground and analyzed for concentrations of P, base cations and micronutrients (Ca, K, Mg, B, Fe) using Inductively Coupled Plasma spectroscopy (ICP-OES; Therma Jarrel-Ash, IRIS Advantage, Waltham, MA, USA) after microwave digestion in nitric acid solution (CEM MARSXpress; Matthews, NC, USA). Total C and N were determined on dry sample using a combustion-reduction elemental analyzer (Costec Analytical Technologies Inc. Valencia, CA, USA). Cellulose, lignin and sol-C were assayed using sequential digestion of increasing acidity in an Ankom fiber analyzer (Ankom Technology, Macedon, NY, USA) and are presented on an ash-free dry mass basis. Total phenols were measured from the frozen leaf disks colorimetrically using the Folin–Ciocalteau method following extraction in 95% methanol and 48 h dark incubation (Ainsworth & Gillespie, 2007).

2.3. Imaging spectrometer data

Airborne remote sensing data were acquired in August–September 2011, 2012 and 2013 using CAO-AToMS (Table 1, Fig. 3), which includes a high-fidelity visible-to-shortwave Infrared (VSWIR) imaging spectrometer and a dual laser, waveform LiDAR (Asner et al., 2012). We collected the data over each study landscape from an altitude of 2000 m a.g.l., an average flight speed of 55–60 m s^{-1}, and a mapping swath of 1200 m. The VSWIR spectrometer measures spectral radiance in 480 channels spanning the 252–2648 nm wavelength range in 5 nm increments (full-width at half-maximum). The VSWIR has a 34° field-of-view and an instantaneous field-of-view of 1 mrad. At 2000 m a.g.l., the VSWIR data collection provided 2.0 m ground sampling distance, or pixel size, throughout each study landscape. The LiDAR has a beam divergence set to 0.5 mrad, and was operated at 200 kHz with 17° scan half-angle from nadir, providing swath coverage similar to the VSWIR spectrometer. Because the airborne data were collected along

Table 1
Descriptive information for 79 1-hectare field plots used for calibration and validation of Carnegie Airborne Observatory (CAO) spectroscopic remote sensing of canopy chemical traits and leaf mass per area. Site abbreviations are given followed by the number of plots within each site. Sites are organized by the year they were imaged by the CAO. Soil orders follow the U.S. Department of Agriculture (USDA) soil taxonomy system.

Year mapped	Site	Soil order	Elevation (m)	MAP (mm)	MAT (°C)
2011	SUC-01; 1	Ultisol	116	2754	26.2
	ALP-01; 1	Ultisol	131	2760	26.3
	JEN-11; 1	Ultisol	131	2700	26.6
	SUC-05; 1	Ultisol	132	2754	26.2
	JEN-12; 1	Entisol	135	2700	26.6
	ALP-30; 1	Entisol	142	2760	26.3
	CUZ-03; 1	Inceptisol	205	2600	24.7
	TAM-06; 1	Inceptisol	215	2600	24.0
	TAM-09; 1	Inceptisol	220	2600	24.0
	TAM-05; 1	Ultisol	223	2600	24.0
	PJL-01; 1	Ultisol	420	5000	23.1
	PJL-02; 1	Entisol	632	5000	23.1
	SPD-02; 1	Inceptisol	1527	4628	18.5
	SPD-01; 1	Inceptisol	1776	4341	18.5
	TRU-08; 1	Inceptisol	1800	4341	18.5
	TRU-04; 1	Inceptisol	2758	2678	13.0
	TRU-03; 1	Inceptisol	3043	2678	13.0
2012					
	ESC-A; 3	Ultisol	945	1055	27.1
	ESC-B; 11	Entisol	945	1055	27.1
2013					
	LA-A; 21	Ultisol	260	2700	24.0
	LA-B; 11	Inceptisol	260	2700	24.0
	SPA; 16	Inceptisol	1500	4628	18.5

adjacent flightlines with 50% overlap, the LiDAR point density was two laser shots m^{-2}, or 8 shots per VSWIR pixel.

The LiDAR data were used to precisely ortho-geolocate the VSWIR data, and to provide a means to mask canopy gaps and shadows, water and exposed soil in the VSWIR data. To achieve this, the laser ranges were combined with the embedded high resolution Global Positioning System-Inertial Measurement Unit (GPS-IMU) data to determine the 3-D locations of laser returns, producing a 'cloud' of LiDAR data. The LiDAR data cloud consists of a very large number of georeferenced point elevation estimates (cm), where elevation is determined relative to a reference ellipsoid (WGS 1984). We used these points to interpolate a raster digital terrain model (DTM) for the ground surface of each landscape. This was achieved using a 10 m × 10 m kernel passed over each flight block, with the lowest elevation estimate in each kernel assumed to be ground. Subsequent points were evaluated by fitting a horizontal plane to each of the ground seed points. If the closest unclassified point was <5.5° and <1.5 m higher in elevation, it was classified as ground. This process was repeated until all points within the block were evaluated. The digital surface model (DSM) was based on interpolations of all first-return points. The measurement of the vertical difference between the DTM and DSM yielded a digital canopy model (DCM) of vegetation height above ground.

The VSWIR data were radiometrically corrected from raw DN values to radiance (W sr^{-1} m^{-2}) using a flat-field correction, radiometric calibration coefficients and spectral calibration data collected in the laboratory. The standardized GPS pulse-per-second measurement was used to precisely co-locate VSWIR spectral imagery to the LiDAR data collection. We created a camera model to determine the three-dimensional location and field-of-view of each sensor element, and combined it with standardized timing information, for data co-registration. A smoothed best estimate of trajectory (SBET), the LiDAR DTM, and the camera model were then used to produce an image geometry model and observational data containing information on solar and viewing geometry for each image pixel. These inputs were used to atmospherically correct the radiance imagery using the ACORN-5 model (Imspec LLC, Glendale, CA, USA). To improve aerosol corrections in ACORN-5, we iteratively ran the model with different visibilities until the reflectance at 420 nm (which is relatively constant for vegetated pixels) was 1%. Reflectance imagery was corrected for cross-track brightness gradients using a bidirectional reflectance distribution function (BRDF) modeling approach described

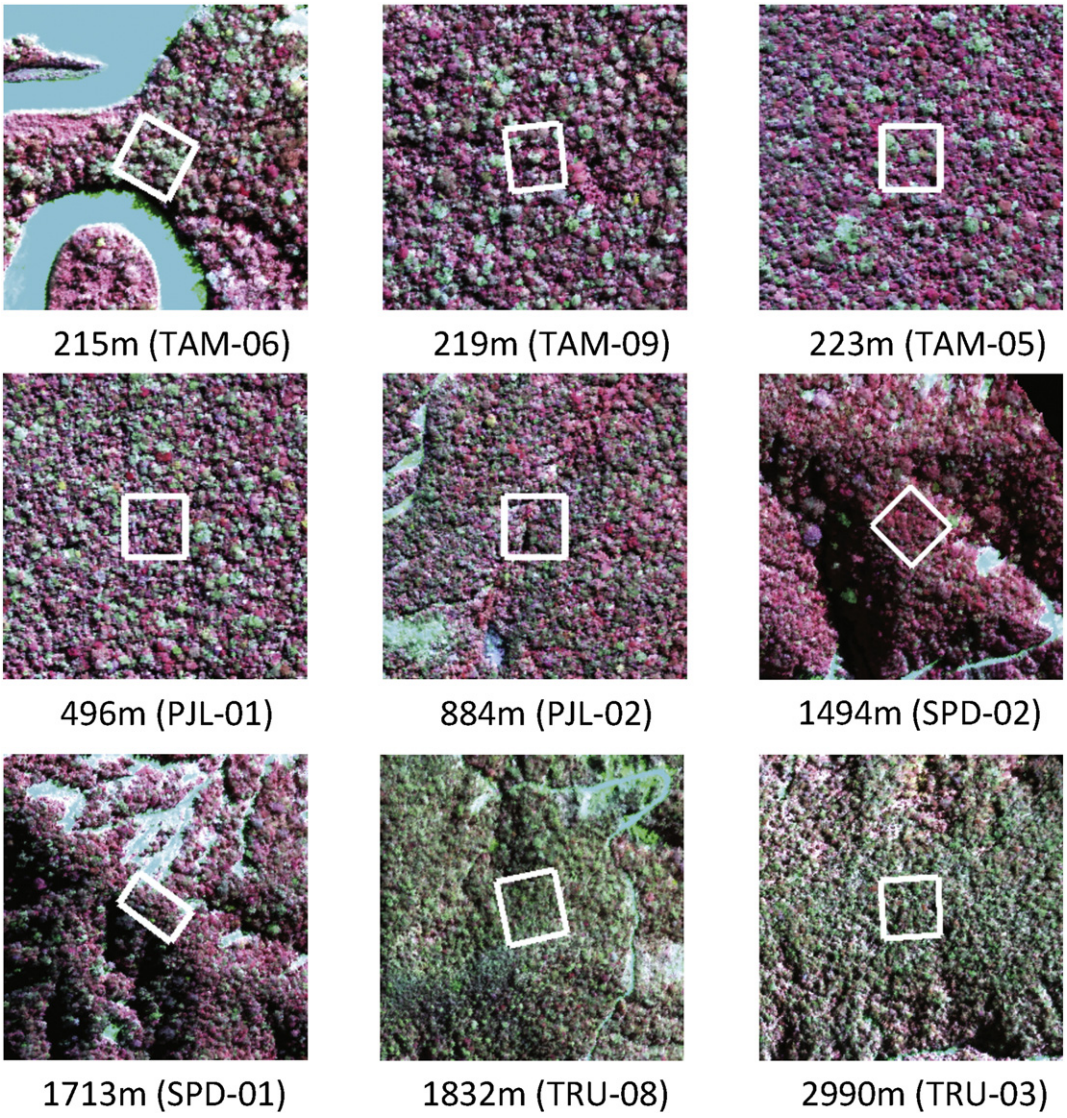

Fig. 3. Examples of color-infrared composite images of Carnegie Airborne Observatory Visible to Shortwave Infrared (VSWIR) imaging spectrometer data of 1-hectare study plots (white boxes) on landscapes ranging from lowland Amazonia to the Andean treeline. Site names and elevations are included in Table 1.

by Colgan, Baldeck, Féret, and Asner (2012). The VSWIR imagery was then orthorectified to the LiDAR DCM.

2.4. Linking field and remotely sensed data

The method for calibration, validation and mapping of canopy chemical traits and LMA is presented in Fig. 4. The goals of the method are to allow for the automated compilation of comparable imaging spectrometer data sets over large geographic areas while minimizing the local-scale effects of sun-sensor-canopy geometry, inter- and intra-crown shading, forest gaps, and terrain-related artifacts. In addition, the method must be compatible with the necessarily sparse sampling of forest canopies in the field.

To achieve this goal, we developed a data-fusion approach facilitated by the collection and inter-calibration of boresight-aligned VSWIR and LiDAR observations. The co-aligned VSWIR and LiDAR data were processed together to develop a suitability map for leaf trait estimation at a prescribed grid cell size (Fig. 4). We selected 1-hectare resolution grid cells to match the size of many typical forest field plots (Peacock, Baker, Lewis, Lopez-Gonzalez, & Phillips, 2007), and the spectral signature of each 1-hectare cell was derived by averaging the spectra of all 2-meter resolution VSWIR measurements that passed the following filtering criteria: (i) Normalized Difference Vegetation Index (NDVI) ≥ 0.8; (ii) vegetation height ≥ 2.0 m; and (iii) minimal intra- or inter-canopy shade in the VSWIR pixel. Through detailed survey of more than 7 million ha of VSWIR imagery over Andean and Amazonian forests, we have found that a minimum NDVI threshold of 0.8 is highly conservative, allowing most tropical canopy foliage into the trait analysis, while excluding areas of un-foliated canopy. The 2-meter minimum height requirement removes bare ground and short non-forest

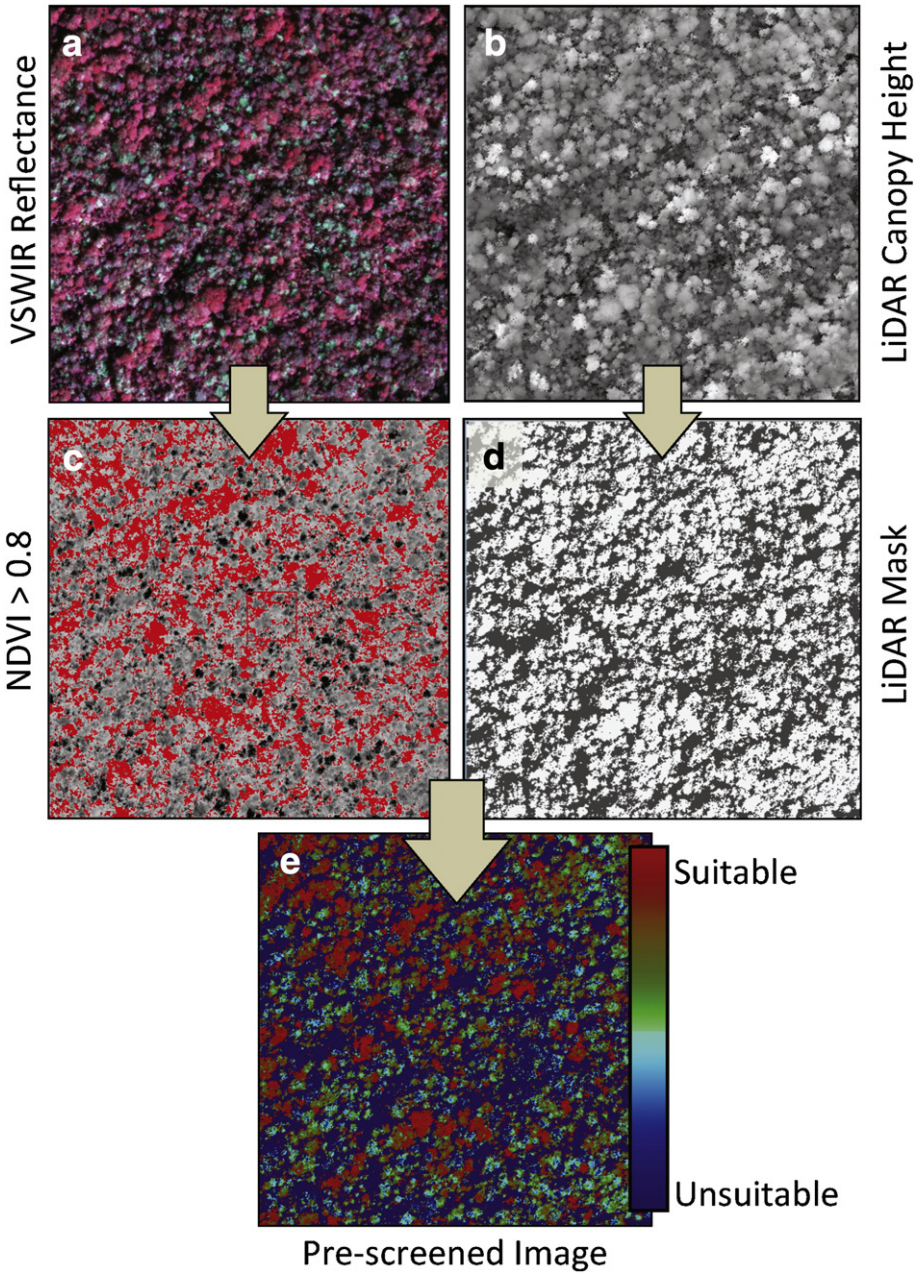

Fig. 4. Pre-screening of (a) CAO Visible-to-Shortwave Infrared (VSWIR) imaging spectrometer data using (b) embedded Light Detection and Ranging (LiDAR) data on canopy height and gaps. (c) Minimum NDVI threshold of 0.8 ensures sufficient foliar cover in each analysis pixel. (d) Combining LiDAR and solar-viewing geometry, a mask is generated to remove pixels in shade, and ground and water surfaces. (e) The resulting suitability image provides an indication of pixels that can be used for chemometric analysis. Here we only used pixels in the top 50% of the suitability index.

vegetation such as exposed grass cover. The shade mask is derived from a ray tracing model that precisely identifies canopy location in unshaded and unobstructed view of the VSWIR spectrometer (Asner et al., 2007). This LiDAR-based shade mask removes VSWIR pixels that are fully or partially shaded by adjacent foliage, branches or crowns. Together, these filters provided a pixel-by-pixel (2.0 m) suitability map within each 1-hectare grid cell, from which average spectral reflectance was computed (Fig. S2). This filtering technique has the advantage of reducing the total canopy analysis area to a level analogous to the "sunlit canopy foliage" criterion often used in field collections of forest canopy foliage. However, it also removes within-plot variation in canopy spectral reflectance properties, which may be considered important in other higher spatial resolution (<1 ha) studies.

A histogram reporting the fraction of the forest canopy that passed through the filtering process in each of the 79 1-hectare plots is shown in Fig. 5a. The mean value for suitable VSWIR sampling in each 1-hectare plot was 52%. In contrast, on average only 5% of each plot was covered by canopies that were sampled in the field (Fig. 5b). This inherent mismatch in scale cannot be directly overcome due to the extreme difficulty of field sampling. However, by creating similar sampling conditions for field-accessible and remotely sensed portions of full-sunlight, highly foliated canopies in each plot, the scale-gap between these disparate data types was effectively minimized.

Following the preparation of the filtered VSWIR reflectance spectra (Fig. 6), we convolved them to 10-nm bandwidth and applied a brightness-normalization adjustment (Fig. S1). Brightness normalization utilizes 'spectral angle' to mitigate differences in brightness that may arise from internal canopy shade, which is proportional to LAI (Kruse et al., 1993; Myneni, Ross, & Asrar, 1989). This reduces the contribution of varying LAI to chemometric determinations of foliar traits from remotely sensed data (Feilhauer, Asner, Martin, & Schmidtlein, 2010). The resulting spectra were trimmed at the far ends (<410 nm, >2450 nm) of the measured wavelength range, as well as in regions dominated by atmospheric water vapor (1350–1480, 1780–2032 nm).

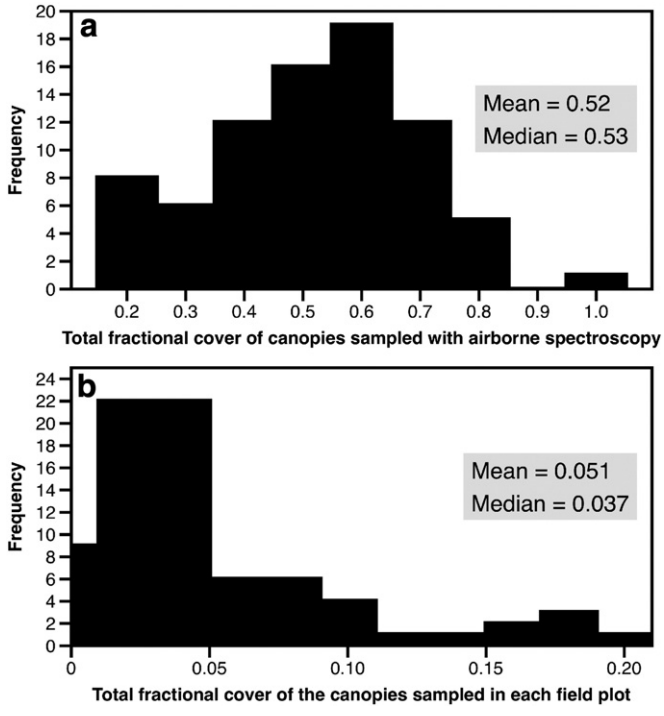

Fig. 5. (a) Histogram showing the fraction of 2-meter CAO VSWIR pixels that passed the pre-screening criteria (Fig. 4) in each of the 79 1-hectare field plots. On average, only 52% of the 2500 VSWIR pixels per hectare were considered appropriate for spectroscopic analysis. (b) Histogram showing the fraction of each 1-hectare plot represented in the field-based canopy sampling effort. On average, just 3–5% of the area of the plots could be sampled in the field due to the inaccessibility of tall tropical forest canopies.

We used Partial Least Squares Regression (PLSR; Haaland & Thomas, 1988) to quantitatively link the airborne VSWIR spectroscopy to field-collected, lab-assayed foliar traits. The PLSR approach is beneficial because it utilizes the continuous spectrum as a single measurement rather than in a band-by-band type of analysis (Boulesteix & Strimmer, 2006; Martens, 2001). To avoid statistical over-fitting, the number of orthogonal spectral dimensions or vectors used in the PLSR analysis was estimated by minimizing the Prediction Residual Error Sum of Squares (PRESS) statistic (Chen, Hong, Harris, & Sharkey, 2004). The PRESS statistic was calculated through a leave-one-out cross-validation procedure for each PLSR model that was run. This cross-validation procedure iteratively generates N − 1 regression models while reserving the rest of the sample from the input data set until the root mean squared error (RMSE) for the PRESS statistic is minimized. The precision and accuracy of the PLSR model for each foliar trait were assessed based on the coefficient of determination (R^2) and the RMSE, respectively, between remotely sensed and field-measured trait values.

To test the robustness and repeatability of the PLSR–PRESS approach with 1-hectare resolution filtered and brightness-normalized VSWIR data, we split the 79 forest plots into calibration (n = 55) and validation (n = 24) subsets each spanning the range of trait values. To minimize model redundancy, we randomly selected 70% of the plots from the 55 plots to generate the PLSR models. For each iteration and leaf trait, the PLSR-PRESS method was run 1000 times on the calibration data to determine producer-based calibration precision and accuracy (Serbin, Singh, McNeil, Kingdon, & Townsend, 2014). The PLSR equations resulting in robust models (R^2 > the mean value of the 1000 iterations) were then used to estimate each canopy trait in the 24 validation plots. This provided a way to calculate a mean and standard deviation of each remotely sensed trait as compared against the field-based value.

3. Results

3.1. Canopy chemical variation

The foliar chemistry and LMA of sunlit canopy trees and lianas spanned a very wide range of values at both site and regional scales (Tables 2, S2–S4). Our range of values meets that which has been reported in global and cross-biome synthesis studies (Poorter, Niinemets, Poorter, Wright, & Villar, 2009; Wright et al., 2004), as well as in a much larger Andes and Amazon canopy chemical data set (Asner, Martin, et al., 2014). By covering a broad range of chemical diversity among taxa and across sites, we had a sufficient data set to adequately test the general relationships between foliar traits and imaging spectroscopy for humid tropical forests.

3.2. Calibration

The 1-hectare filtered and brightness-normalized VSWIR data calibrated well against a suite of foliar traits representing light capture and growth, structure and defense, and maintenance and metabolism (Table 2). All light capture and growth traits, including chlorophyll a + b, carotenoids, N, P, LMA, water and soluble C showed excellent calibration performances, with R^2 = 0.55–0.71 and %RMSE = 5–16%, where %RMSE is calculated in terms of the original value for each trait as 100 * $RMSE_{trait}$ / μ_{trait}. Variances among the 1000 PLSR model runs were about 8–18%, both in terms of R^2 and RMSE. The number of spectral (latent) vectors selected among the 1000 PLSR model iterations was also consistent.

Among the structure-defense traits, lignin and total C were calibrated with the highest precision (R^2 = 0.54–0.71) and accuracy (%RMSE = 2.7–14.9%) (Table 2). Individual calibration runs indicated a wider range of performances as compared with those involving the light capture and growth traits. Phenols and cellulose, however, had weaker calibration performances, and yet remained highly significant ($p < 0.001$). For foliar maintenance-metabolism traits, Ca performed

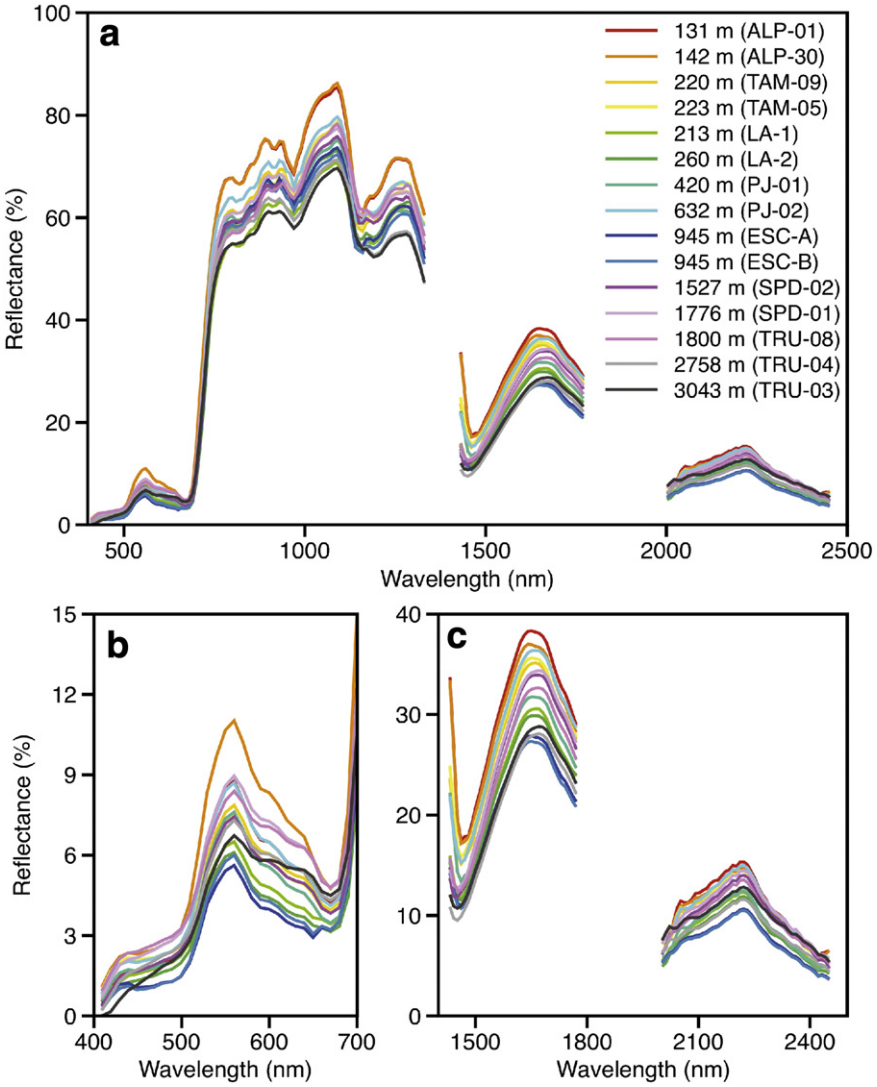

Fig. 6. (a) Examples of canopy reflectance spectra derived from the mean number of pixels suitable for chemometric analysis following pre-screening within each 1-hectare plot. Zoom images of spectra are provided for (b) visible and (c) shortwave-infrared regions to reveal subtle features associated with varying chemical concentrations.

the best in terms of precision ($R^2 = 0.79 \pm 0.17$) and accuracy (%RMSE = 16.9%) (Table 2). Other cation calibrations were highly significant ($p < 0.001$), but exhibited lower precision and accuracy. We found that the number of latent spectral vectors automatically selected among the 1000 model runs varied narrowly for most traits, with a few exceptions such as for Ca and total C. Greater variation in the number of latent vectors indicates instability in the spectral-to-chemical relationships among model runs.

The standardized PLSR coefficients indicated that all wavelength regions were important for most of the foliar traits (Fig. 7). In this figure, departures from the zero-line indicate spectral features that are most important in determining the foliar trait of interest. There was consistency in the spectral regions required for chlorophyll a + b, carotenoid and N calibrations as indicated in the correlation between PLSR weightings (Table S5). Specifically, the visible region along the 700-nm 'red edge' and in the blue (400–500 nm) proved to be important contributors to the PLSR models for these traits. There were also important contributions from the shortwave-IR region, particularly in the 1500–1700 nm range, indicative of protein–N interactions with solar radiation (Curran, 1989).

We also found that the visible and shortwave-IR were critical to the estimation of P, LMA, soluble C and water (Fig. 7). However, for these traits, the near-IR played an additionally important role, particularly in the 1000–1300 nm range. Moreover, the 2000–2500 nm range contributed to the calibration of the spectral data to LMA and soluble C. The other chemistries representing structure-defense and maintenance-metabolism trait groups had regression coefficients that also required multiple spectral features across the 400–2500 nm wavelength range. None of the chemical traits had the same spectral weightings, and the vast majority of chemical traits required portions of the spectrum in combinations that were not highly correlated among PLSR coefficients (Table S5), suggesting a unique role of each trait in determining the spectral reflectance measured from the VSWIR spectrometer.

3.3. Validation

Validation models indicated highly significant results for all traits, with the exception of K ($p < 0.001$; Table 3). The best performances were achieved for photosynthetic pigments, N, P, LMA, Fe and total C. Regressed against field data, their R^2 values ranged from 0.39–0.58 and %RMSE of 14–34%. A somewhat lower performing group in terms of precision included water, soluble C, lignin and cellulose, although their relative accuracies remained relatively high (%RMSE = 6–24%). The poorest performers were phenols and base cations (%RMSE = 24–63%).

Table 2
Calibration of canopy chemical traits and leaf mass per area (LMA) using airborne high-fidelity visible-to-shortwave infrared (VSWIR) spectroscopy. Mean ± standard deviation of PLSR model results (R^2; RMSE) calculated randomly selected field plots containing the canopy trait range shown.

	R^2	RMSE	%RMSE	Vectors	Trait range
Light capture and growth					
Chlorophyll ab* (mg g^{-1})	0.70 ± 0.07	0.84 ± 0.10	15.66	5 (1)	2.65–8.53
Carotenoids* (mg g^{-1})	0.63 ± 0.08	0.16 ± 0.02	13.15	5 (1)	0.69–1.84
N* (%)	0.54 ± 0.09	0.30 ± 0.03	14.47	5 (1)	1.28–3.33
P* (%)	0.71 ± 0.10	0.02 ± 0.00	16.59	6 (2)	0.06–0.26
LMA* (g m^{-2})	0.69 ± 0.08	11.87 ± 1.55	9.99	5 (2)	76.0–180.0
Water (%)	0.49 ± 0.13	2.95 ± 0.38	5.22	5 (2)	44.3–63.9
Soluble carbon (%)	0.49 ± 0.14	4.40 ± 0.87	9.16	4 (3)	36.0–71.9
Structure and defense					
Phenols (mg g^{-1})	0.33 ± 0.10	20.30 ± 1.77	18.37	1 (1)	51.0–156.2
Lignin (%)	0.51 ± 0.15	3.51 ± 0.62	14.94	3 (2)	9.2–33.5
Cellulose (%)	0.38 ± 0.12	2.33 ± 0.34	14.34	3 (3)	8.2–21.7
Total carbon (%)	0.69 ± 0.16	1.35 ± 0.35	2.67	6 (3)	42.1–54.6
Maintenance and metabolism					
Ca** (%)	0.79 ± 0.17	0.14 ± 0.06	16.99	9 (5)	0.04–2.96
B* (μg g^{-1})	0.53 ± 0.07	7.31 ± 0.89	43.33	5 (1)	4.74–55.98
Fe* (μg g^{-1})	0.56 ± 0.09	12.39 ± 1.94	27.29	4 (1)	21.8–120.1
K* (%)	0.42 ± 0.22	0.15 ± 0.04	24.57	4 (3)	0.36–1.51
Mg* (%)	0.34 ± 0.19	0.06 ± 0.01	31.78	3 (3)	0.07 – 0.50

RMSE = root mean square error in units of the original chemical assays.
%RMSE = RMSE expressed as a percentage of the mean value of the leaf trait.
R^2 = regression coefficient for K-fold cross-validation data used during PLSR analyses.
Vectors = number of spectral weighting vectors, or orthogonal degrees of freedom, from the VSWIR data used for the chemical determination.
* Indicates that chemical values were natural log-transformed for PLSR analysis.
** Square-root of chemical value.

4. Discussion

We have found that a suite of canopy foliar chemical traits and LMA can be estimated using airborne high-fidelity visible-to-shortwave infrared (VSWIR) imaging spectroscopy. Because field techniques are often severely under-sample foliar traits in forests, thereby struggling to provide systematic, repeat estimates of canopy properties at the stand level, imaging spectroscopy can greatly reduce the inherent limitations and sampling biases associated with field work. This issue has been particularly problematic in tall statured, floristically complex tropical forests, where data quality continues to go mostly unmonitored, and where geographic sampling biases limit the interpretability of plot-network data.

4.1. Observing conditions for remote sensing of functional traits

Remote sensing of canopy chemistry is not a new idea, and enormous progress has been made since the late 1980s toward the goal of developing sensors and techniques to remotely probe the chemical content of vegetation (Homolová, Malenovsky, Clevers, García-Santos, & Schaepman, 2013; Kokaly et al., 2009; Martin, Plourde, Ollinger, Smith, & McNeil, 2008; Ustin et al., 2009; Wessman, 1992). However, the convolution of vegetation structure, foliar chemistry and observation geometry (sun and sensor) has also impeded progress in understanding how best to isolate foliar chemistry within remotely sensed data. Variation in canopy structure, particularly LAI, leaf angle distribution, and within-canopy gaps can dominate optical reflectance signatures (Asner, 1998). There also often exists spatial covariance of canopy structure and chemistry (Ollinger, 2011). Moreover, current canopy reflectance models will, virtually by their formulation, simulate a diminished effect of foliar chemistry on spectral-optical signatures, particularly in the near-infrared (Knyazikhin et al., 2013), but this is largely an artifact of the inability of current models to simulate the multiple chemical constituents that drive foliar spectral properties, especially in the shortwave-infrared (Curran, 1989; Feret et al., 2008; Jacquemoud et al., 2009).

The best chance to isolate the effects of foliar traits on canopy reflectance signatures relies on reducing the relative contribution of canopy structure, and by controlling for solar and viewing geometry. Reliable plant functional trait mapping can be achieved by pre-screening portions of the canopy for gaps, low LAI, and shadows. While low LAI portions of the canopy can be removed with a simple NDVI filter, gaps and shadows require more detailed structural information. Asner and Martin (2008) first showed how LiDAR can effectively be used for this task, but only if the LiDAR data are tightly aligned with the spectrometer data to provide precise sun-to-canopy-to-sensor geometry for every pixel (Asner et al., 2012). This technique, combined with LiDAR-derived minimum vegetation height data, results in a suitability map at high spatial resolution (e.g., 2 m) within which the most appropriate spectral data can be selected for chemometric analysis (Fig. 4). By carrying out these steps, the pre-screened vegetation canopies become more comparable over large tracts of otherwise highly variable canopy structural and terrain conditions.

In this study, the NDVI ≥0.8 filter was conservative, allowing into the calibration and validation at least 95% of the canopy data within the 79 1-hectare field plots spread throughout Amazonian and the Andean forests (data not shown). The 2-meter minimum height filter removed water bodies, clearings, landslide areas, and large gaps. The majority of the filtering, however, was driven by the LiDAR-derived intra- and inter-crown shade masks. Using this approach, our calibration and validation underwent enormous filtering down to about 52% of each forest plot, but with wide variation between plots (20–100%; Fig. 5a).

Beyond the spatial filtering approach used here, additional measures can be taken to maximize the expression of foliar traits in imaging spectrometer data. One approach is brightness normalization, which helps reduce the contribution of varying LAI and foliar clumping on canopy spectral reflectance (Feilhauer et al., 2010). Through brightness normalization of the VSWIR spectra that passed the spatial filtering step, the expression of foliar traits should be maximized. Our pre-screening and brightness normalization approach facilitated the calibration of multiple foliar chemical traits and LMA against VSWIR imaging spectrometer

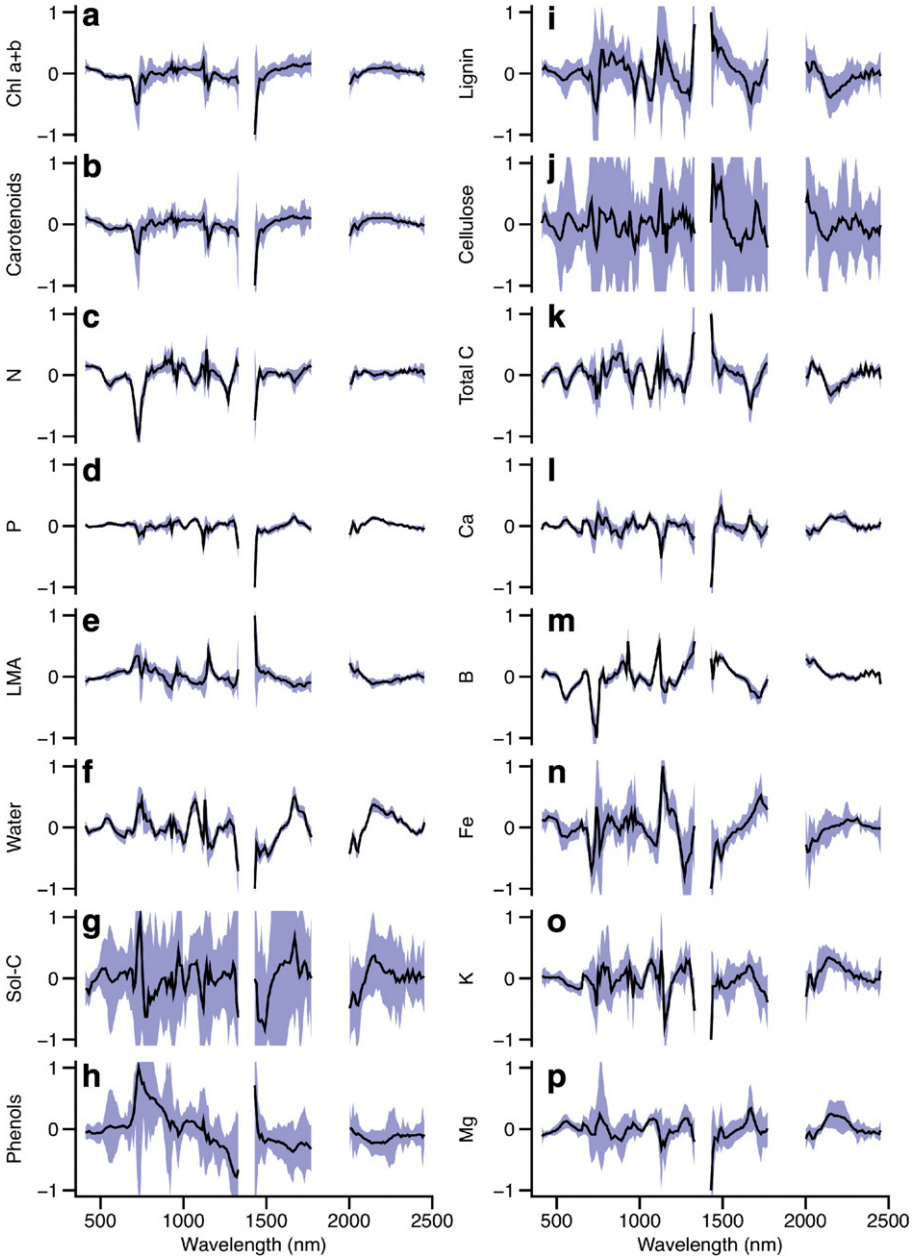

Fig. 7. Mean and standard deviation of spectral weighting vectors for PLSR chemometric results for 1000 iterations reported in Table 2. (a) Chlorophyll a + b (chl a + b); (b) carotenoids; (c) nitrogen; (d) phosphorus, (e) leaf mass per area (LMA); (f) water; (g) soluble carbon (sol-C), (h) phenols; (i) lignin; (j) cellulose, (k) total carbon; (l) calcium; (m) boron; (n) iron; (o) potassium; (p) magnesium.

data (Table 2). Rarely has a suite of foliar traits been calibrated against airborne imaging spectrometer data, and the demonstrably high performance is due to three interacting factors. First, as stated, pre-screening and brightness normalization reduces noise caused by variable canopy structure and shade. Second, our field-collected foliar trait data also controlled for full sunlight canopy position, so the field data were made radiometrically and biologically more compatible with the filtered VSWIR data. Third, our field data span the range of known canopy chemical variation in terrestrial plants. The issue of chemical range in the PLSR methodology cannot be over-emphasized; a wide chemical input range is required in a similar way to the requirements of laboratory assay calibrations (Martens, 2001). Our canopy chemical data cover an enormous range of values, reflecting evolutionary processes that have led to the diversification of species and communities on contrasting geologic substrates and climatic conditions across the western Amazon (Asner, Martin, et al., 2014).

4.2. Assessing remote sensing performance

The calibration exercise revealed highly significant quantitative linkages between VSWIR spectroscopy and a suite of foliar functional traits that mediate light capture, growth, structure, defense, maintenance and metabolism. Model calibration performances varied depending upon the random selection of input field plots, and are in general agreement with previous PLSR calibration studies at both leaf and canopy scales (Curran, 1989; Knox et al., 2011; Kokaly et al., 2009; Martin & Aber, 1997; Martin et al., 2008; Peterson et al., 1988; Skidmore et al., 2010; Ustin et al., 2009). Our random model selection approach provided a

Table 3
Independent field validation of canopy chemical traits and leaf mass per area (LMA) using airborne high-fidelity visible-to-shortwave infrared (VSWIR) spectroscopy. Mean ± standard deviation of validation statistics are reported.

	R^2	RMSE	%RMSE
Light capture and growth			
Chlorophyll ab* (mg g^{-1})	0.58 ± 0.05	1.50 ± 0.71	28.14
Carotenoids* (mg g^{-1})	0.49 ± 0.06	0.25 ± 0.08	21.20
N* (%)	0.48 ± 0.05	0.31 ± 0.06	15.19
P* (%)	0.39 ± 0.05	0.04 ± 0.03	34.86
LMA* (g m^{-2})	0.53 ± 0.05	22.88 ± 6.46	19.25
Water (%)	0.34 ± 0.05	3.86 ± 0.44	6.83
Soluble carbon (%)	0.34 ± 0.04	6.89 ± 2.19	14.33
Structure and defense			
Phenols (mg g^{-1})	0.04 ± 0.01	26.60 ± 1.99	24.07
Lignin (%)	0.26 ± 0.04	5.65 ± 1.16	24.08
Cellulose (%)	0.20 ± 0.04	3.42 ± 1.92	21.04
Total carbon (%)	0.44 ± 0.04	3.09 ± 0.43	6.09
Maintenance and metabolism			
Ca** (%)	0.52 ± 0.08	0.50 ± 0.11	33.34
B* (μg g^{-1})	0.30 ± 0.07	9.64 ± 1.88	57.12
Fe* (μg g^{-1})	0.48 ± 0.04	12.27 ± 5.41	27.03
K* (%)	0.05 ± 0.02	0.33 ± 0.43	55.66
Mg* (%)	0.21 ± 0.06	0.09 ± 0.04	45.45

RMSE = root mean square error in units of the original chemical assays.
%RMSE = RMSE expressed as a percentage of the mean value of the leaf trait.
R^2 = regression coefficient for field validation data.
* Indicates that chemical values were natural log-transformed for PLSR analysis.
** Square-root of chemical value.

way to track stability and repeatability during calibration, and to forecast performance in validation. Doing so revealed that most light-capture and growth traits, as well as total C, lignin and Ca, produce the most consistent and accurate calibrations (Table 2). In contrast, random selection indicated that most base cations (e.g., K, Mg, B, Fe) and phenols showed more erratic calibration behavior. Interestingly, %RMSE values were the better predictor of how well the chemicals would be estimated during the validation phase of the study. This strongly suggests that accuracy (RMSE) is the better analytical metric of performance than is R^2, or precision, which is under-emphasized in the ecological and remote sensing literature (Homolová et al., 2013; Townsend et al., 2003).

Despite the high-precision calibrations of many foliar traits to airborne VSWIR spectroscopy, the validation exercise proved more challenging to interpret in terms of user-based performance. Experimenting with the field and airborne data, we feel that a validation accuracy of 25% relative RMSE or lower indicates very good performance. This is particularly true given the relative high per-sample and project-level uncertainty of field and laboratory studies of foliar traits (Townsend, Asner, & Cleveland, 2008; Vitousek, 1982; Wessman, Aber, Peterson, & Melillo, 1988a), and particularly given the extreme spatial and biological mismatches between field and remotely sensed measurements inherent in this study (Fig. 5). Even given our stringent pre-screening for full sunlit, highly foliated canopies in the VSWIR data, the mismatch to the field estimates of canopy traits remained large. Limitations of local access to particular crowns within the canopy are common, especially if the protocol focuses on obtaining samples from fully sunlit portions of the canopy. Tropical forests are spatially complex, multi-layered structures that cannot be easily reached from the ground. Relatively extreme climbing techniques are needed in remote forests such as those incorporated into this study, and in the end, sometimes only a few crowns can be accessed in an entire hectare of forest. At other times, the foliage from many canopies can be acquired (up to 38 in one of our field plots). We also note that both the field and remotely sensed data were collected over a period of three years, reflecting the realities of field work in remote regions of the tropics. Different combinations of the 2011, 2012, and 2013 airborne data likely did not temporally match the field data during the random selection of plots used in the validation models. Inter-annual variation in canopy chemistry and phenology would thus certainly have affected the validation process, especially in the context of model performances.

It is therefore quite surprising to find that the accuracy of most light-capture, growth, structure and defense traits fell in the <25% error category (Table 3). This finding strongly suggests that controlling for sunlit canopies provides a unique way to bridge the scale-gap between field and spectroscopic measurements at plot to landscape scales. In effect, we used our general ecological knowledge of foliar trait adjustment to average solar illumination conditions (Kitajima, Mulkey, & Wright, 2005; Poorter et al., 2009), as a functional scaling link between handpicked foliage collections and plot-scale remote sensing observations. Our method, which reflects the realities of doing field and remote sensing work in conditions of very high biodiversity and high structural heterogeneity, has evolved over years of trial and error in the field and from the air. It is thus likely to be repeatable and scalable to other vegetation types and imaging spectrometers, including future spaceborne instruments.

4.3. Next steps

Using a novel combination of VSWIR imaging spectroscopy and LiDAR data from the Carnegie Airborne Observatory, we have shown that multiple foliar chemical traits and LMA can be estimated for Amazonian and Andean forests. These forested regions remain almost completely unexplored and inaccessible to scientific study, and thus we must continue to work toward methods that greatly extend the limited capabilities of sparse field plots, which inherently cannot capture the geographic pattern of functional trait variation.

Further testing of the methods presented here will be required before the approach can be made operational with other airborne and future spaceborne imaging spectrometers. However, we do note that the absolute and relative performance of each chemical trait and LMA calibration with the CAO VSWIR spectrometer data closely mirrored the model-predicted performances derived from a worldwide collection of foliar chemical and spectral data (Asner et al., 2011). Correspondence between the results from this study and those using a completely different, globally distributed data set suggests that our approach based on a pre-filtered, VSWIR data can be used in other regions. With the CAO, we intend to use this capability to map canopy functional traits of forests. In the longer-term, a similar approach should be attempted using forthcoming replicas of the Carnegie VSWIR–LiDAR combination, including the new U.S. National Ecological Observatory Network (NEON) airborne systems (Kampe et al., 2010). The NEON systems were designed using CAO specifications and engineering drawings, so the transferability of the approach presented here should be straightforward. Future spaceborne imaging spectrometers such as the European Union's EnMAP and the proposed NASA HyspIRI (Stuffler et al., 2007) should be capable of utilizing a subset or modification of our approach, for example, by utilizing minimum NDVI and/or fractional canopy cover estimation as a pre-filtering step before chemometric study of the Earth's ecosystems.

Acknowledgments

We thank R. Tupayachi, F. Sinca, L. Carranza-Jimenez, N. Jaramillo, P. Martinez, and other contributors to the Carnegie Spectranomics Project. We thank P. Townsend and an anonymous reviewer for comments that greatly improved the manuscript. This study was funded by the John D. and Catherine T. MacArthur Foundation and the endowment of the Carnegie Institution for Science. The Carnegie Airborne Observatory is made possible by the Avatar Alliance Foundation, Margaret A. Cargill Foundation, John D. and Catherine T. MacArthur Foundation, Grantham Foundation for the Protection of the Environment, W.M. Keck Foundation, Gordon and Betty Moore Foundation, Mary Anne Nyburg Baker and G. Leonard Baker Jr., and William R. Hearst III.

Appendix A. Supplementary data

Supplementary data to this article can be found online at http://dx.doi.org/10.1016/j.rse.2014.11.011.

References

Achard, F., Beuchle, R., Mayaux, P., Stibig, H. -J., Bodart, C., Brink, A., et al. (2014). Determination of tropical deforestation rates and related carbon losses from 1990 to 2010. *Global Change Biology*, 2540–2554.

Ainsworth, E.A., & Gillespie, K.M. (2007). Estimation of total phenolic content and other oxidation substrates in plant tissues using Folin–Coicalteau reagent. *Nature Protocols*, *2*, 875–877.

Asner, G.P. (1998). Biophysical and biochemical sources of variability in canopy reflectance. *Remote Sensing of Environment*, *64*, 234–253.

Asner, G.P. (2008). Hyperspectral remote sensing of canopy chemistry, physiology and diversity in tropical rainforests. In M. Kalacska, & G.A. Sanchez-Azofeifa (Eds.), *Hyperspectral remote sensing of tropical and subtropical forests* (pp. 261–296). Boca Raton, Fl: Taylor and Francis Group.

Asner, G.P., Anderson, C., Martin, R.E., Knapp, D.E., Tupayachi, R., Kennedy-Bowdoin, T., et al. (2014). Landscape-scale changes in forest structure and functional traits along an Andes-to-Amazon elevation gradient. *Biogeosciences*, *11*, 843–856.

Asner, G.P., & Green, R.O. (2001). Imaging spectroscopy measures desertification in the Southwest U.S. and Argentina. *EOS Transactions*, *82*, 601–606.

Asner, G.P., Knapp, D.E., Boardman, J., Green, R.O., Kennedy-Bowdoin, T., Eastwood, M., et al. (2012). Carnegie Airborne Observatory-2: Increasing science data dimensionality via high-fidelity multi-sensor fusion. *Remote Sensing of Environment*, *124*, 454–465.

Asner, G.P., Knapp, D.E., Kennedy-Bowdoin, T., Jones, M.O., Martin, R.E., Boardman, J., et al. (2007). Carnegie airborne observatory: In-flight fusion of hyperspectral imaging and waveform light detection and ranging for three-dimensional studies of ecosystems. *Journal of Applied Remote Sensing*, *1*, 013536.

Asner, G.P., & Martin, R.E. (2008). Spectral and chemical analysis of tropical forests: Scaling from leaf to canopy levels. *Remote Sensing of Environment*, *112*, 3958–3970.

Asner, G.P., & Martin, R.E. (2011). Canopy phylogenetic, chemical and spectral assembly in a lowland Amazonian forest. *New Phytologist*, *189*, 999–1012.

Asner, G.P., Martin, R.E., Knapp, D.E., Tupayachi, R., Anderson, C., Carranza, L., et al. (2011). Spectroscopy of canopy chemicals in humid tropical forests. *Remote Sensing of Environment*, *115*, 3587–3598.

Asner, G.P., Martin, R.E., Tupayachi, R., Anderson, C.B., Sinca, F., Carranza-Jimenez, L., et al. (2014). Amazonian functional diversity from forest canopy chemical assembly. *Proceedings of the National Academy of Sciences*, *111*, 5604–5609.

Atkinson, P.M., Foody, G.M., Curran, P.J., & Boyd, D.S. (2000). Assessing the ground data requirements for regional scale remote sensing of tropical forest biophysical properties. *International Journal of Remote Sensing*, *21*, 2571–2587.

Baccini, A., Goetz, S.J., Walker, W.S., Laporte, N.T., Sun, M., Sulla-Menashe, D., et al. (2012). Estimated carbon dioxide emissions from tropical deforestation improved by carbon-density maps. *Nature Climate Change*, http://dx.doi.org/10.1038/nclimate1354.

Boulesteix, A. -L., & Strimmer, K. (2006). Partial least squares: A versatile tool for the analysis of high-dimensional genomic data. *Briefings in Bioinformatics*, *8*, 32–44.

Chambers, J.Q., Asner, G.P., Morton, D.C., Anderson, L.O., Saatchi, S.S., Espirito-Santo, F.D.B., et al. (2007). Regional ecosystem structure and function: Ecological insights from remote sensing of tropical forests. *Trends in Ecology & Evolution*, *22*, 414–423.

Chapin, F.S., III (1991). Integrated responses of plants to stress. *BioScience*, *41*, 29–36.

Chen, S., Hong, X., Harris, C.J., & Sharkey, P.M. (2004). Sparse modeling using orthogonal forest regression with PRESS statistic and regularization. *IEEE Transactions on Systems, Man, and Cybernetics*, *34*, 898–911.

Coley, P.D., Kursar, T.A., & Machado, J. -L. (1993). Colonization of tropical rain forest leaves by epiphylls: Effects of site and host-plant leaf lifetime. *Ecology*, *74*, 619–623.

Colgan, M., Baldeck, C., Féret, J. -B., & Asner, G. (2012). Mapping savanna tree species at ecosystem scales using support vector machine classification and BRDF correction on airborne hyperspectral and LiDAR data. *Remote Sensing*, *4*, 3462–3480.

Cuevas, E., & Medina, E. (1988). Nutrient dynamics within amazonian forests II. Fine root growth, nutrient availability and leaf litter decomposition. *Oecologia*, *76*, 222–235.

Curran, P.J. (1989). Remote sensing of foliar chemistry. *Remote Sensing of Environment*, *30*, 271–278.

Demarty, M., Morvan, C., & Thellier, M. (1984). Calcium and the cell wall. *Plant, Cell and Environment*, *7*, 441–448.

Evans, J.R. (1989). Photosynthesis and nitrogen relationships in leaves of C_3 plants. *Oecologia*, *78*, 9–19.

Feilhauer, H., Asner, G.P., Martin, R.E., & Schmidtlein, S. (2010). Brigthness-normalized partial least squares regression for hyperspectral data. *Journal of Quantitative Spectroscopy and Radiative Transfer*, *111*, 1947–1957.

Feret, J. -B., François, C., Asner, G.P., Gitelson, A.A., Martin, R.E., Bidel, L.P.R., et al. (2008). PROSPECT-4 and 5: Advances in the leaf optical properties model separating photosynthetic pigments. *Remote Sensing of Environment*, *112*, 3030–3043.

Fyllas, N., Patiño, S., Baker, T., Bielefeld Nardoto, G., Martinelli, L., Quesada, C., et al. (2009). Basin-wide variations in foliar properties of Amazonian forest: Phylogeny, soils and climate. *Biogeosciences*, *6*, 2677–2708.

Gerard, F.F., & North, P.R.J. (1997). Analyzing the effect of structural variability and canopy gaps on forest BRDF using a geometric–optical model. *Remote Sensing of Environment*, *62*, 46–62.

Girardin, C.A.J., Malhi, Y., AragÃO, L.E.O.C., Mamani, M., Huaraca Huasco, W., Durand, L., et al. (2010). Net primary productivity allocation and cycling of carbon along a tropical forest elevational transect in the Peruvian Andes. *Global Change Biology*, *16*, 3176–3192.

Goetz, A.F.H., Vane, G., Solomon, J.E., & Rock, B.N. (1985). Imaging spectrometry for Earth remote sensing. *Science*, *228*, 1147–1153.

Green, R.O., Eastwood, M.L., Sarture, C.M., Chrien, T.G., Aronsson, M., Chippendale, B.J., et al. (1998). Imaging spectroscopy and the airborne visible infrared imaging spectrometer (AVIRIS). *Remote Sensing of Environment*, *65*, 227–248.

Haaland, D.M., & Thomas, E.V. (1988). Partial least-squares methods for spectral analyses. 1. Relation to other quantitative calibration methods and the extraction of qualitative information. *Analytical Chemistry*, *60*, 1193–1202.

Homolová, L., Malenovsky, Z., Clevers, J.G.P.W., García-Santos, G., & Schaepman, M.E. (2013). Review of optical-based remote sensing for plant trait mapping. *Ecological Complexity*, *15*, 1–16.

Jacquemoud, S., Verhoef, W., Baret, F., Bacour, C., Zarco-Tejada, P.J., Asner, G.P., et al. (2009). PROSPECT plus SAIL models: A review of use for vegetation characterization. *Remote Sensing of Environment*, *113*, S56–S66.

Kampe, T.U., Asner, G.P., Green, R.O., Eastwood, M., Johnson, B.R., & Kuester, M. (2010). Advances in airborne remote sensing of ecosystem processes and properties — Toward high-quality measurement on a global scale. In W. Gao, T.J. Jackson, & J. Wang (Eds.), *Remote sensing and modeling of ecosystems for sustainability VII* (pp. 7809). Proc. SPIE.

Kitajima, K., Mulkey, S.S., & Wright, S.J. (2005). Variation in crown light utilization characteristics among tropical canopy trees. *Annals of Botany*, *95*, 535–547.

Knox, N.M., Skidmore, A.K., Prins, H.H.T., Asner, G.P., van der Werff, H.M.A., de Boer, W.F., et al. (2011). Dry season mapping of savanna forage quality, using the hyperspectral Carnegie Airborne Observatory sensor. *Remote Sensing of Environment*, *115*, 1478–1488.

Knyazikhin, Y., Schull, M.A., Stenberg, P., MÃµttus, M., Rautiainen, M., Yang, Y., et al. (2013). Hyperspectral remote sensing of foliar nitrogen content. *Proceedings of the National Academy of Sciences*, *110*, E185–E192.

Kokaly, R.F., Asner, G.P., Ollinger, S.V., Martin, M.E., & Wessman, C.A. (2009). Characterizing canopy biochemistry from imaging spectroscopy and its application to ecosystem studies. *Remote Sensing of Environment*, *113*, S78–S91.

Kruse, F.A., Lefkoff, A.B., Boardman, J.B., Heidebrecht, K.B., Shapiro, A.T., Barloon, P.J., et al. (1993). The spectral image processing system (SIPS) — Interactive visualization and analysis of imaging spectrometer data. *Remote Sensing of Environment*, *44*, 145–163.

Martens, H. (2001). Reliable and relevant modelling of real world data: A personal account of the development of PLS Regression. *Chemometrics and Intelligent Laboratory Systems*, *58*, 85–95.

Martin, M.E., & Aber, J.D. (1997). High spectral resolution remote sensing of forest canopy lignin, nitrogen, and ecosystem processes. *Ecological Applications*, *7*, 431–444.

Martin, M.E., Plourde, L.C., Ollinger, S.V., Smith, M. -L., & McNeil, B.E. (2008). A generalizable method for remote sensing of canopy nitrogen across a wide range of forest ecosystems. *Remote Sensing of Environment*, *112*, 3511–3519.

Melillo, J.M., Aber, J.D., & Muratore, J.F. (1982). Nitrogen and lignin control of hardwood leaf litter decomposition dynamics. *Ecology*, *63*, 621–626.

Myneni, R.B., & Asrar, G. (1993). Radiative transfer in three-dimensional atmosphere–vegetation media. *Journal of Quantitative Spectroscopy and Radiative Transfer*, *49*, 585–598.

Myneni, R.B., Ross, J., & Asrar, G. (1989). A review on the theory of photon transport in leaf canopies. *Agricultural and Forest Meteorology*, *45*, 1–153.

Ollinger, S.V. (2011). Sources of variability in canopy reflectance and the convergent properties of plants. *New Phytologist*, *189*, 375–394.

Peacock, J., Baker, T.R., Lewis, S.L., Lopez-Gonzalez, G., & Phillips, O.L. (2007). The RAINFOR database: Monitoring forest biomass and dynamics. *Journal of Vegetation Science*, *18*, 535–542.

Peterson, D.L., Aber, J.D., Matson, P.A., Card, D.H., Swanberg, N., Wessman, C., et al. (1988). Remote sensing of canopy and leaf biochemical contents. *Remote Sensing of Environment*, *24*, 85–108.

Poorter, H., Niinemets, U., Poorter, L., Wright, I.J., & Villar, R. (2009). Causes and consequences of variation in leaf mass per area (LMA): A meta-analysis. *New Phytologist*, *182*, 565–588.

Reich, P.B., Ellsworth, D.S., & Uhl, C. (1995). Leaf carbon and nutrient assimilation and conservation in species of differing successional status in an oligotrophic Amazonian forest. *Functional Ecology*, *9*, 65–76.

Samanta, A., Ganguly, S., Hashimoto, H., Devadiga, S., Vermote, E., Knyazikhin, Y., et al. (2010). Amazon forests did not green-up during the 2005 drought. *Geophysical Research Letters*, *37*, L05401.

Serbin, S.P., Singh, A., McNeil, B.E., Kingdon, C.C., & Townsend, P.A. (2014). Spectroscopic determination of leaf morphological and biochemical traits for northern temperate and boreal tree species. *Ecological Applications*, *24*, 1651–1669.

Simonson, W.D., Coomes, D.A., & Burslem, D.F.R.P. (2014). Forests and global change: An overview. In D.A. Coomes, D.F.R.P. Burslem, & W.D. Simonson (Eds.), *Forests and global change* (pp. 1–19). Cambridge, U.K.: Cambridge University Press.

Skidmore, A.K., Ferwerda, J.G., Mutanga, O., Van Wieren, S.E., Peel, M., Grant, R.C., et al. (2010). Forage quality of savannas — Simultaneously mapping foliar protein and polyphenols for trees and grass using hyperspectral imagery. *Remote Sensing of Environment*, *114*, 64–72.

Souza, C., Roberts, D.A., & Cochrane, M.A. (2005). Combining spectral and spatial information to map canopy damages from selective logging and forest fires. *Remote Sensing of Environment*, *98*, 329–343.

Stuffler, T., Kaufmann, C., Hofer, S., Förster, K.P., Schreier, G., Mueller, A., et al. (2007). The EnMAP hyperspectral imager — An advanced optical payload for future applications in Earth observation programmes. *Acta Astronautica*, *61*, 115–120.

Townsend, A.R., Asner, G.P., & Cleveland, C.C. (2008). The biogeochemical heterogeneity of tropical forests. *Trends in Ecology and the Environment*, *23*, 424–431.

Townsend, P.A., Foster, J.R., Chastain, R.A., & Currie, W.S. (2003). Application of imaging spectroscopy to mapping canopy nitrogen in the forests of the central Appalachian Mountains using Hyperion and AVIRIS. *IEEE Transactions on Geoscience and Remote Sensing*, *41*, 1347.

Tuomisto, H., Poulsen, A.D., Ruokolainen, K., Moran, R.C., Quintana, C., Celi, J., et al. (2003). Linking floristic patterns with soil heterogeneity and satellite imagery in Ecuadorian Amazonia. *Ecological Applications*, *13*, 352–371.

Ustin, S.L., Gitelson, A.A., Jacquemoud, S., Schaepman, M., Asner, G.P., Gamon, J.A., et al. (2009). Retrieval of foliar information about plant pigment systems from high resolution spectroscopy. *Remote Sensing of Environment*, *113*(Supplement 1), S67–S77.

Ustin, S.L., Roberts, D.A., Gamon, J.A., Asner, G.P., & Green, R.O. (2004). Using imaging spectroscopy to study ecosystem processes and properties. *Bioscience*, *54*, 523–534.

Vitousek, P.M. (1982). Nutrient cycling and nutrient use efficiency. *American Naturalist*, *119*, 553–572.

Wessman, C.A. (1992). Imaging spectrometry for remote sensing of ecosystem processes. *Advances in Space Research*, *12*, 7361–7368.

Wessman, C.A., Aber, J.D., Peterson, D.L., & Melillo, J.M. (1988a). Foliar analysis using near infrared reflectance spectroscopy. *Canadian Journal of Forest Research*, *18*, 6–11.

Wessman, C.A., Aber, J.D., Peterson, D.L., & Melillo, J.M. (1988b). Remote sensing of canopy chemistry and nitrogen cycling in temperate forest ecosystems. *Nature*, *335*, 154–156.

Wright, I.J., Reich, P.B., Westoby, M., Ackerly, D.D., Baruch, Z., Bongers, F., et al. (2004). The worldwide leaf economics spectrum. *Nature*, *428*, 821–827.